Modelling approaches for chiral chromatography on polysaccharide-based and macrocyclic antibiotic chiral selectors: A review

De Gauquier, Pieter; Vanommeslaeghe, Kenno; Vander Heyden, Yvan ; Mangelings, Debby

Published in:
Analytica Chimica Acta

DOI:
10.1016/j.aca.2021.338861

Publication date:
2022

Modelling Approaches for Chiral Chromatography on Polysaccharide-based and Macrocyclic Antibiotic Chiral Selectors: a Review

Author names and affiliations

Pieter De Gauquier, Kenno Vanommeslaeghe, Yvan Vander Heyden, Debby Mangelings

Vrije Universiteit Brussel (VUB), Department of Analytical Chemistry, Applied Chemometrics and Molecular Modelling, Laarbeeklaan 103, 1090 Brussels, Belgium.

Corresponding author: Debby Mangelings; E-mail address: Debby.Mangelings@vub.be; tel.: +32(0)24774329

Abstract

An overview of molecular modelling approaches, related to chiral separations on polysaccharide-based and macrocyclic antibiotic chiral selectors, is presented. Both atomistic calculations and empirical fitting procedures are discussed. Atomistic calculations, such as docking and molecular dynamics can be used to model the interactions between enantiomers and the chiral stationary phase. This may help obtaining information about the chiral recognition mechanism. Conversely, in empirical fitting procedures, mathematical models for relevant separation parameters are fitted to experimental observations. The latter use theoretical molecular descriptors, calculated from the molecular structure, which are combined into a model to predict a given response, for example, retention. Such relationships, when used in chiral separations, are often called quantitative structure enantioselective retention relationships (QSERR) and an increased interest in them can be observed in the literature. Different regression models are discussed, such as multiple linear regression and partial least squares.

Keywords

Chiral chromatography; Chiral stationary phases; Molecular dynamics; Molecular docking; Empirical fitting procedures

Abbreviations

ACMPC: amylose tris-(3-chloro-5-methylphenylcarbamate; ACPC: amylose tris-(3-chlorophenylcarbamate); ADMPC: amylose tris-(3,5-dimethylphenylcarbamate); ANN: artificial neural networks; AP: Carhart atom pair; CCMPC: cellulose tris-(3-chloro-5-methylphenylcarbamate); CD: circular dichroism; CDCC: conformation-dependent chirality codes; CDCPC: cellulose tris-(3,5-dichlorophenylcarbamate); CDMPC: cellulose tris-(3,5-dimethylphenylcarbamate); CMPA: chiral mobile-phase additives; CSP: chiral stationary phase(s); DA: discriminant analysis; DPLS1: discriminant partial least squares for one categorical response variable; GA: genetic algorithms; GAFF: general AMBER force field; LFER: linear free-energy relationships; LSER: linear solvation energy relationships; MD: molecular dynamics; MIA: multivariate image analysis; MIF: molecular interaction fields; MLR: multiple linear regression; MOE_2D: molecular operating environment_2D; PCFF: polymer consistent force field; PCR: principal component regression; PEF: potential energy function; PLS: partial least squares regression; POSC: polar organic solvents chromatography; QSERR: quantitative structure enantioselective retention relationships; QSPR: quantitative structure property relationships; QuBiLS-MAS: Quadratic, Bilinear and N-Linear mapS - Matrices and Atomic weightingS; RF: random forest; RMSE: root mean square error; SCAR: structure chiral activity relationships; TOMOCOMD-CARDD: topological molecular computer design – computer-aided rational drug design;

1. Introduction

Any chiral molecule has a mirror-image counterpart, its enantiomer, on which it cannot be superposed. In other words, enantiomers are a special case of stereo-isomers, with the same atoms arranged into different three-dimensional structures. However, being mirror images, enantiomers have identical physicochemical properties, except for their optical rotations and their behaviour in asymmetric environments [1]. As biological environments are asymmetric, enantiomers generally exhibit different biological activities in organisms [1, 2]. As a consequence nowadays enantiopure drugs, i.e. drugs containing only one enantiomer, became more important as they should be preferentially developed over racemates [3]. The regulatory agencies around the world introduced guidelines to separately evaluate racemates and enantiomers [4].

In a drug development stage, an enantiopure drug may be obtained by asymmetric synthesis or by separation of a racemic mixture [3]. Since both enantiomers have to be investigated separately, each enantiomer might be synthesized, but it is typically easier to develop a synthetic pathway for the racemic mixture and to separate both enantiomers with a chiral separation method [5]. As a consequence separation techniques became very important to resolve enantiomers from a racemic mixture, both for analytical and (semi-)preparative purposes [1, 5]. To separate enantiomers, chiral chromatographic techniques are the most often applied.

In liquid chromatography, three approaches to separate enantiomers exist: (1) the indirect approach; (2) the direct approach with addition of chiral mobile-phase additives (CMPA), and (3) the direct approach using chiral stationary phases (CSP). For more information about these approaches we refer to [6].

Within the chromatographic approaches, supercritical fluid chromatography (SFC) is increasingly applied for enantioseparations for analytical and preparative purposes. The mobile phase in SFC contains supercritical carbon dioxide (CO_2), which is inflammable, cheap and non-toxic. Moreover, in the specific context of preparative chromatography, less time and

energy are necessary to evaporate the mobile phase, because the amount of co-solvent used in SFC is very low and usually methanol. Finally, CO_2 can be separated from the co-solvent and recycled [7, 8].

Hundreds of CSP are already synthesized by different research groups, but two classes are the most important for chiral separations: polysaccharide CSP (*Figure 1*), introduced by Okamoto et al. [9, 10, 11], and macrocyclic antibiotic CSP (*Figure 2*), developed by Armstrong et al. [12]. They both have broad chiral recognition abilities. More information about these selectors can be found in [6, 13, 14, 15].

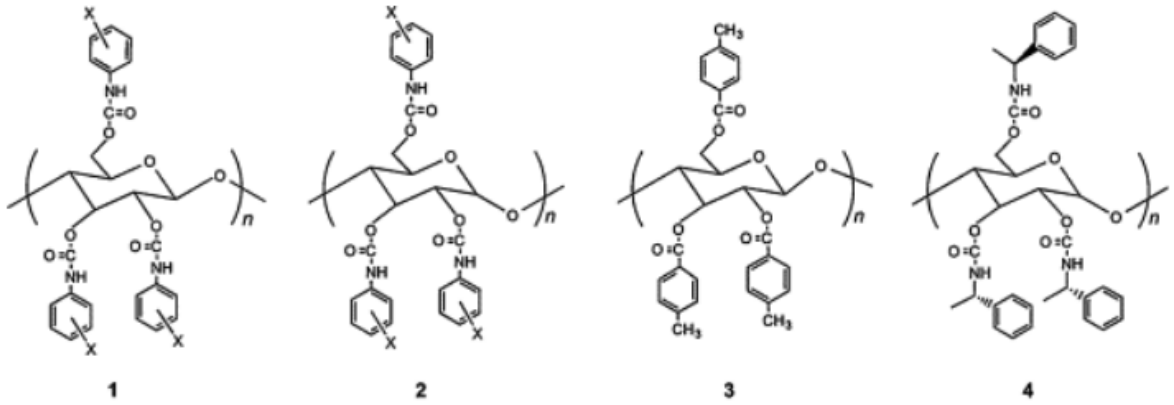

Figure 1. Different types of polysaccharide CSP. Reproduced with permission from [16].

X = a: 3,5-$(CH_3)_2$; b: 3,5-Cl_2; c: 3-Cl; d: 3-Cl-4-CH_3.

(1a): cellulose tris-(3,5-dimethylphenylcarbamate); **(1b):** cellulose tris-(3,5-dichlorophenylcarbamate); **(2a):** amylose tris-(3,5-dimethylphenylcarbamate); **(2b):** amylose tris-(3,5-dichlorophenylcarbamate); **(2c):** amylose tris-(3-chlorophenylcarbamate); **(2d):** amylose tris-(3-chloro-4-methylphenylcarbamate); **(3):** cellulose tris-(4-methylbenzoate); **(4):** amylose tris-[(S)-α-methylbenzylcarbamate].

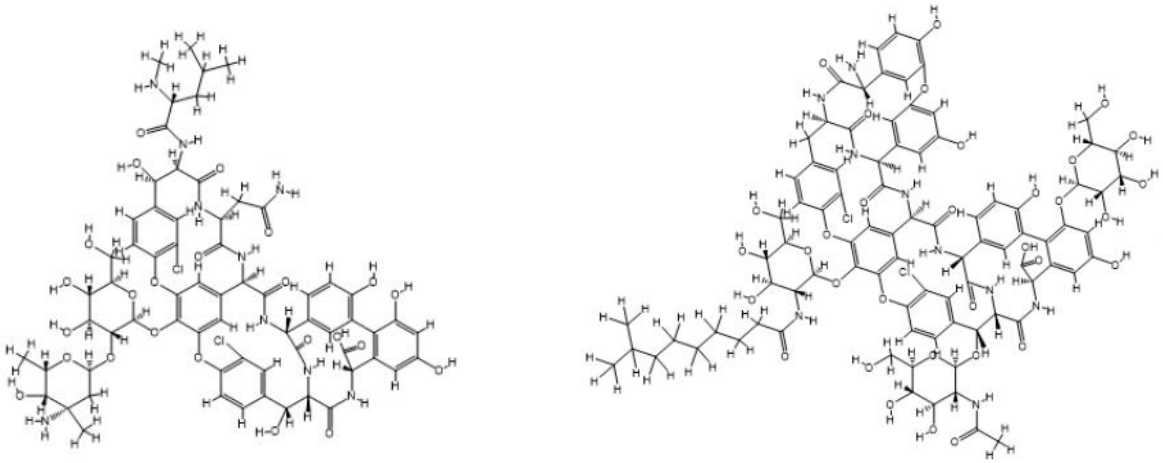

Figure 2. Macrocyclic antibiotic CSP: vancomycin (left) and teicoplanin (right). Reproduced with permission from [17].

The chiral recognition mechanisms for both polysaccharide and macrocyclic antibiotic CSP are still not fully understood, despite much research has already been dedicated to it [6, 18, 19, 20]. Interactions important for both the general retention and for the enantioseparation exist between enantiomers and CSP [13]. When considering retention, hydrophobic interactions (π-π interactions) are important in reversed-phase elution mode, whereas in normal phase and polar organic elution mode, hydrophilic interactions (hydrogen-bonds) are pertinent. Although multiple types of interactions may be considered in case of enantioseparations [21].

For polysaccharide CSP, the most important interactions are hydrogen-bonds with the carbamate groups and π-π interactions with the phenyl rings. The latter are on the outside of the polysaccharide chain, forming grooves in which the carbamate groups are embedded [20, 21]. Furthermore, Peluso et al. [22, 23, 24, 25] investigated the role of halogen bonds, which seem to be important in the chiral recognition process. These are electrostatic interactions, which arise from the anisotropic electron distribution around covalently bonded halogen atoms. Macrocyclic antibiotic selectors contain a peptidic core with terminal carboxylic acid and amine groups. These groups are ionized at a certain pH and may interact with compounds through ionic interactions. These selectors contain also four fused macrocyclic rings (except vancomycin which contains three) embedded by several aromatic groups, hydroxyl functions and sugar units (except the teicoplanin aglycone selector), which are responsible for π-π

interactions (aromatic rings), hydrogen-bonds (hydroxyl functions), dipole-dipole interactions, steric hindrance and London dispersion interactions [18].

The chiral recognition mechanisms of high-molecular weight selectors have been studied using spectroscopic methods, such as nuclear magnetic resonance (NMR) and infrared (IR) spectroscopy [26]. Because of the different binding sites with diverse affinities for enantiomers, it is difficult to determine the selector structures in the solid state and in solution. In addition, popular chiral selectors often exhibit solubility problems in several solvents and/or do not show chiral discrimination in solvents in which they are soluble. Therefore, computational methods are often employed to supplement the experimental data [26]. However, for polysaccharide and macrocyclic antibiotic selectors, the elucidation of the chiral recognition mechanism and the prediction of chiral separations remains challenging.

Apart from the use of molecular modelling approaches to gain fundamental insight in the chiral recognition mechanism, models may also help predicting separation parameters. Indeed, while the separation of enantiomers is important in many fields of industrial and pharmaceutical research, the selection of a suitable chromatographic system (chiral selector and mobile phase) is not trivial. As a consequence, chiral method development requires considerable experimentation and is often highly demanding with respect to time, material and labour. The use of adequate models may be an advantage as they would allow selecting a suitable chromatographic system to obtain an enantioseparation [27]. However, many types of interactions are important when considering high-molecular weight selectors. Therefore a structurally diverse test set has to be used to be able to construct suitable models.

Two different types of models can be distinguished: empirical fitting procedures and atomistic models. Fitting procedures are generally based on a regression model, which is used to find a correlation between physical, chemical or biological properties on the one hand and molecular descriptors that are derived from the molecular structure on the other hand. Conversely, atomistic models in a general sense attempt to quantify the energetics of all the interactions

between the atoms in the analytes and the chiral selectors. Both molecular docking and molecular dynamics (MD) [28] belong in this category.

Recently, Sardella et al. [29] reviewed atomistic calculations of the last four decades to explain the enantiomer elution sequence on both low- and high-molecular weight selectors.

In contrast, the present review focuses on applications of molecular modelling approaches in enantioseparations on high-molecular weight selectors, i.e. polysaccharides and macrocyclic antibiotics, and differentiates from the above review by the inclusion of not only atomistic calculations, but also empirical fitting procedures to predict enantioselectivity, besides the application of atomistic calculations, covering the period 2015 - 2020.

2. Molecular calculations

2.1 Molecular Dynamics

The first step of any MD simulation is the construction of a molecular system, which in this context would consist of a chiral selector, a large number of solvent molecules, and optionally one or more analyte molecules. In this system, the thermal motions of all atoms are simulated on a short time scale – typically in the order of 10 ns to 10 µs. This is done by numerically integrating Newton's equations of motion, which requires knowledge of the forces on all the atoms. Such forces are typically obtained from an empirical force field, which represents the potential energy surface of a molecule using simplified mathematical functions [30, 31].

The force fields most commonly used for simulations involving biomolecules represent the system with a so-called "Class I additive Potential Energy Function" (PEF). Such PEFs require large numbers of parameters determining the forces between chemically bonded atoms (chemical bonds, atomic angles and dihedral angles (rotations about a bond)), and forces between non-bonded atoms (Van der Waals interactions and electrostatic interactions) [32].

Accordingly, a force field is the totality of its PEF and its parameter set, and the latter is essentially what distinguishes the commonly used biomolecular force fields and the different

versions thereof [33, 34]. Popular examples are AMBER [35], CHARMM [36, 37], GROMOS [32, 33, 38] and OPLS [34].

Until recently, atomistic studies of chromatographic separations and chiral separations were limited to static calculations that took neither the solvent effect nor the fact that the process of enantiorecognition in chromatography is dynamic into account [39]. Conversely, in this section, we will consider true MD studies that include the solvent effect and the dynamic process of enantiorecognition during chromatographic separation; static calculations are deferred to §2.2 (Molecular Docking).

In MD simulations, solvents can be treated either explicitly or implicitly [40]. In explicit-solvent simulations, the simulation system includes thousands of solvent molecules, whereas implicit-solvent methods treat the solvent as a continuum. This is significantly less accurate, but historically, this sped up the simulation by reducing the number of particles in the system. However, trends in processor architecture have weakened this performance advantage, precipitating a rise in popularity of explicit solvent simulations.

Table 1 contains a summary of recent papers that applied MD simulations to chiral separations.

Table 1. Summary of recent MD simulations performed using different analytes and CSP.

Analytes	CSP [(1)]	Force Field / medium	Year (reference)
Pyrazole derivatives	Cellulose tris-(4-methylbenzoate)	Polymer consistent force field (PCFF) / 7 different dielectric constants	2016 [41]
Flavanone	ADMPC	General AMBER force field (GAFF) / explicit-solvent (methanol; heptane/IPA (90/10 v/v))	2017 [1]
10 chiral molecules	ADMPC	GAFF / explicit-solvent (methanol; heptane/IPA (90/10 v/v); acetonitrile)	2019 [39]
8 chiral halogenated 4,4'-bipyridines	CDMPC, ADMPC	GAFF / explicit-solvent (n-hexane)	2018 [42]

4 chiral molecules	ADMPC	GAFF / explicit-solvent (methanol; heptane/IPA (90/10 v/v))	2020 [2]
Carnosine enantiomers	Teicoplanin A2-2	OPLSe / explicit-solvent (methanol/water (60/40 v/v))	2020 [43]

(1) ADMPC: amylose tris-(3,5-dimethylphenylcarbamate), CDMPC: cellulose tris-(3,5-dimethylphenylcarbamate)

ADMPC is a widely used selector and many groups performed research to elucidate its recognition mechanism. ADMPC has a helical structure where the carbamate groups are located inside the grooves of the polymer and the phenyl groups on the outside of the polymer chain [1].

Zhao et al. [1] used explicit-solvent atomistic MD simulations to investigate the effect of the used solvents on the chiral recognition mechanism of ADMPC for flavanone enantiomers. Methanol and heptane/isopropanol (90/10 v/v) were used as solvent systems and it was observed that the dimensions of ADMPC differ depending on the solvent. The ADMPC helix is longer in heptane/isopropanol (90/10 v/v) than in methanol. In addition, the hydrogen-bonding lifetime between the CSP and flavanone enantiomers was determined. For both solvents the hydrogen-bonding lifetime was found higher for the S enantiomer, which corresponds with the experimental results, where a longer retention of the S enantiomer was observed. When comparing the selectivity in both solvent systems, it was observed that the selectivity was lower in heptane/isopropanol (90/10 v/v) than in methanol.

Wang et al. [39] used explicit-solvent atomistic MD simulations to investigate the dynamic interaction between ADMPC and enantiomers, as well as the effects of different solvents (methanol, heptane/isopropanol (90/10 v/v) and acetonitrile) on both. In *Figure 3*, an example of possible interactions for benzoin enantiomers can be observed. A metric to predict the elution sequence of the enantiomers, which correlates with the ratio of their retention times, was also proposed. It was based on the hydrogen-bond lifetime, since long-living hydrogen-

bonds between enantiomer and CSP slow down the passage through the CSP, while the opposite is seen when weak hydrogen-bonds are formed. The experimental elution sequence could be explained very well in both simulated solvents.

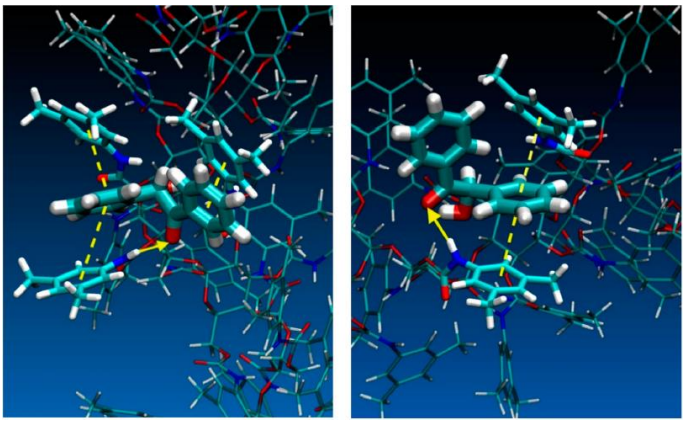

Figure 3. Snapshot of an MD simulation for the R (right image) and S (left image) enantiomers of benzoin on an ADMPC CSP. Both enantiomers show multiple interactions with CSP: ring-ring interactions (dashed line) and hydrogen-bond interactions (arrow from donor to acceptor). Reproduced with permission from [39].

In a follow-up study, the same research group [2] built a model consisting of multiple ADMPC strands coated on an amorphous silica surface to have a more representative model for the real CSP and the interactions with the enantiomers. Explicit-solvent fully atomistic MD simulations were again used to investigate the interactions between ADMPC, enantiomers and solvents. The results of these improved models were more consistent with experimental elution sequences and separation factors.

Another group [41] studied the effect of temperature and solvent on a cellulose tris-(4-methylbenzoate) CSP using pyrazole derivatives. They investigated the interaction energy between the enantiomers and CSP using different dielectric constants as a coarse approximation for the effects of different solvents. Under polar eluent conditions, the R enantiomer eluted last, which was attributed to a stronger relative contribution of apolar interactions to the binding energy. Under non-polar conditions the elution sequence changed,

with the S enantiomer eluting as last, caused by stronger polar interactions. The difference in interaction energy at different temperatures was less significant than the solvent effect.

Recently, halogen-bond interactions between enantiomers and cellulose-based CSP have been described [22]. A halogen bond is a non-covalent interaction in which an electron-rich region of an acceptor atom is attracted to a region of positive electrostatic potential that occurs on single-bonded halogen atoms opposite to the atom they are bonded to [24]. Peluso et al. [42] investigated this phenomenon in a MD study using nonamer (9-mer) ADMPC and CDMPC selectors, as halogen-bond acceptors in an n-hexane box resembling normal-phase liquid chromatography (NPLC) conditions. The aim of this study was to obtain more insights into the halogen-bond-driven chiral separations. Eight halogenated 4,4'-bipyridines were investigated on both selectors and 37,5% and 75% of the experimental elution sequences obtained with ADMPC and CDMPC, respectively, were explained. *Figure 4* shows an example of a simulation of the occupancy of 2,2',3,3',5,5'-hexaiodo-4,4'-bipyridine in a groove of CDMPC. The last eluted enantiomer showed a deeper insertion into the CDMPC selector, whereas the first eluted enantiomer is more present at the surface. This is in accordance with the experimental results and generally demonstrates that halogen-bond interactions could cooperate in enantiorecognition processes driven by π-π or hydrogen-bond interactions.

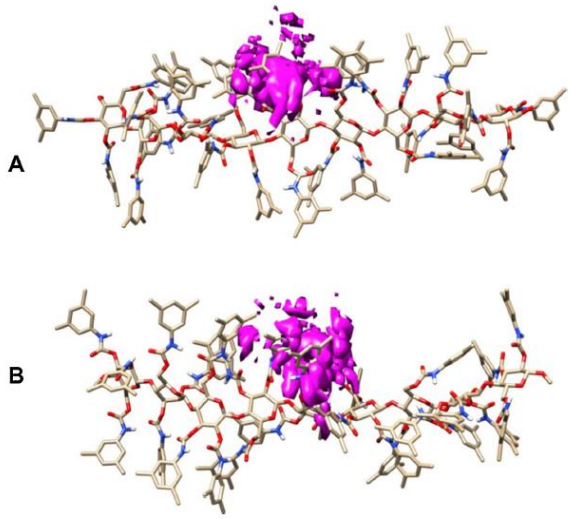

Figure 4. MD simulation of the occupancy of 2,2',3,3',5,5'-hexaiodo-4,4'-bipyridine in a groove of CDMPC: (A) complex with first eluted enantiomer; (B) complex with last eluted enantiomer [42].

Sardella et al. [43] performed MD simulations to study the chiral recognition mechanism of carnosine, a dipeptide, on a teicoplanin A2-2 selector. The number of hydrogen-bonds between (S)-carnosine and the selector was found to be higher than with (R)-carnosine, but this was not the case for charge-charge and cation-π interactions. During the MD trajectory, the most important interactions identified between the enantiomers and the selector were hydrogen-bond and ionic interactions. The difference in retention time between both enantiomers, and the later elution of the R enantiomer, was explained by the observation that (R)-carnosine engaged in one more charge-charge interaction with the selector than the corresponding S enantiomer. These results were in accordance with those obtained in reference [44] in reversed-phase liquid chromatography (RPLC) conditions and a teicoplanin A2-2 selector.

2.2 Molecular Docking

In the context of chiral separations, molecular docking calculations are to study the interaction between the CSP (receptor) and both enantiomers (ligands) by approximately predicting the binding geometries and ranking the binding affinities of the enantiomers binding to the CSP [13]. It involves two steps: prediction of the conformation of the enantiomers in the binding site of the selector (“posing”) and estimation of the binding affinity (“ranking” or “scoring”). Since there are many possible conformations, sampling algorithms are developed to “sample” different conformations of the molecules in the selector [45]. Subsequently, scoring functions are applied to rank all conformations based on the binding affinity between ligand and receptor [45].

The most commonly used software for studying interactions between enantiomers and chiral selectors is AutoDock [13]. Although older docking programs typically kept the receptor immobile, more recent branches of Autodock, specifically AutoDock 4 and AutoDock Vina, allow flexibility of side chains of the receptor [45, 46]. It should however be noted that all current docking programs are highly optimized for protein receptors in an aqueous medium. Thus, applying them on non-protein chiral selectors in a solvent mixture with different properties than

water would be expected to yield less accurate results. Several research groups performed docking calculations to elucidate the chiral recognition mechanism on different types of CSP, as summarized in *Table 2*.

Table 2. Recent docking calculations using different analytes and CSP.

Analytes	CSP [(1)]	Docking software/medium	Year (reference)
Pidotimod	ADMPC	GOLD/vacuum	2015 [47]
16 dipeptide enantiomers	ADMPC	AutoDock 4.2/vacuum	2015 [48]
2 dipeptides	ADMPC	AutoDock 4.2 Vina/vacuum	2015 [49]
4 enantiomers of 5-bromo-3-ethyl-3-(4-nitrophenyl)-piperidine-2,6-dione	ADMPC	AutoDock 4.2/vacuum	2016 [50]
Enantiomers of four 3-aryl-substituted-γ-butyrolactones	ADMPC	AutoDock 4.2/accounted for mobile phase by the use of dielectric constant	2017 [51]
Eight azole antifungals	CDCPC	AutoDock 4.2/vacuum	2018 [52]
Eight anticholinergic drugs	ACPC	AutoDock 4.2/vacuum	2018 [53]
7-[1-alkylpiperidin-3-yl)methoxy]coumarin derivatives	ADMPC	AutoDock 4.2/vacuum	2018 [54]
Six quinolones	Teicoplanin	AutoDock 4.0/vacuum	2018 [55]
Chiral xanthonic derivatives	Teicoplanin, teicoplanin aglycone, vancomycin and ristocetin	AutoDock Vina/vacuum	2018 [17]
Napropamide	ADMPC, CDMPC, CCMPC	Molegro/vacuum	2018 [56]

Five β-adrenergic blockers	CDCPC	AutoDock 4.2/vacuum	2019 [57]
Pantoprazole	Teicoplanin aglycone	AutoDock Vina/vacuum	2019 [58]
Mandelic acid	Vancomycin	AutoDock Vina/vacuum	2020 [59]
Eight psychoactive drugs	Cellulose tris-(4-methylbenzoate)	AutoDock 4.2/vacuum	2020 [60]

(1) CDCPC: cellulose tris-(3,5-dichlorophenylcarbamate), ACPC: amylose tris-(3-chlorophenylcarbamate), CCMPC: cellulose tris-(3-chloro-5-methylphenylcarbamate)

Dou et al. [47] performed docking calculations on an ADMPC selector using pidotimod, a synthetic dipeptide with two chiral centres, to examine the enantiorecognition mechanism. The driving force for enantioseparation seems to be Van der Waals interactions.

Ali et al. [48] performed docking calculations using 16 dipeptides on an ADMPC CSP. Only one of 2 chiral centres was changed, leading to two configurations for each dipeptide, i.e. SS and SR. The docking energy of the SR enantiomer was observed to be more negative than that of the SS enantiomer, although the difference was very small. The SS enantiomer was predicted to elute first, because for the SR enantiomer a stronger interaction with the CSP is expected. The most important interactions were determined to be hydrogen-bond and π-π interactions. Since no experimental results were available, no comparison with experimental results could be made. In a follow-up study, the same research group resolved two dipeptides (DL-alanine-DL-tyrosine & DL-leucine-DL-phenylalanine) on an ADMPC CSP in RPLC mode [49]. The interactions with the CSP were also evaluated using docking calculations to predict the elution sequence. The chromatographic results report that the stereoisomers from both dipeptides eluted in the following sequence: LL, DD, DL, LD. This sequence shows a discrepancy with the docking energies, which were reported the most negative for the LL enantiomer and the least for the LD enantiomer.

In a third paper, the chiral recognition mechanism and elution sequence of four 5-bromo-3-ethyl-(4-nitrophenyl)-piperidine-2,6-dione enantiomers were also studied on an ADMPC

selector [50]. The major forces for chiral recognition were again determined to be hydrogen-bonds and π-π interactions.

Rossi et al. [51] used docking calculations to predict the elution sequence of four γ-butyrolactone derivatives on an ADMPC CSP. The S enantiomer was predicted to elute first for all derivatives due to the weaker binding energies. The R enantiomer showed a better fit in the amylose CSP, with a stronger hydrogen-bond than the S enantiomer.

Zhu et al. [52] studied the interactions of eight azole antifungals with a CDCPC CSP. Differences in binding energies were observed between enantiomers. The differences were determined by the number and strength of the intermolecular interactions with the CSP. For example, in *Figure 5* the docking calculation of both enantiomers of butoconazole is presented. The R enantiomer showed the most negative docking energy, which means that a more stable complex is formed between that enantiomer and the CSP, whereas the S enantiomer showed the least negative docking energy and thus less stable complex with the CSP in agreement with the experimental data. The study also sought to obtain information about the interaction mechanism, pointing to hydrophobic interactions and hydrogen-bonds as the most important interactions.

Li et al. [53] performed calculations for eight anticholinergic drugs on an ACPC CSP to study their recognition mechanism. The binding energies were calculated to predict the interaction strength of each enantiomer with the CSP and those results were in agreement with the experimental data.

Pisani et al. [54] studied the enantiorecognition mechanism of several racemic 7-[1-alkylpiperidin-3-yl)methoxy]coumarin derivatives on an ADPMC CSP, besides building quantitative structure property relationships (QSPR), which are discussed lower. Docking calculations gave better insight in the intermolecular forces that are important for the enantioselective binding of the investigated compounds on the CSP. It was observed that the enantiomers could bind into cavities present in the CSP. The binding was stronger for the S enantiomers than for the R enantiomers. In fact, the 3-NO_2-phenyl group of the S enantiomer is able to go deeper into the CSP ravine, which results in strong π-π and hydrogen-bond

interactions. For the R enantiomer, the 3-NO_2-phenyl group is directed towards the solvent, leading to weaker interactions.

Zhao et al. [57] performed docking calculations on a CDCPC CSP using five beta blockers. Different enantioselectivity values were experimentally seen for these analytes and the study sought to rationalize this with docking calculations. For each pair of enantiomers, the difference in binding energies $\Delta\Delta E$ was determined by subtracting the respective docking scores. This quantity correlated well with the enantioselectivity (α), a measure that gives information about the ability of the chiral stationary phase to discriminate between two enantiomers. For example, (R)-bevantolol (ΔE = -5.96 kcal/mol) and (S)-bevantolol (ΔE = -5.04 kcal/mol) showed the highest $\Delta\Delta E$ value (0.92 kcal/mol), which corresponded to the high observed enantioselectivity. The most important interactions observed were hydrogen-bond interactions and π-π interactions.

As can be concluded from the above, there exists a moderately large body of docking studies for polysaccharide CSP. Conversely, docking studies for macrocyclic antibiotic CSP started appearing more recently. These will be the subject of the remainder of this section.

Ali et al. [55] performed docking calculations on a teicoplanin CSP in RPLC mode using quinolones. The results predicted a stronger interaction with the R enantiomer than with the S enantiomer, and thus a shorter retention of the latter. The most important interactions are hydrogen-bond (due to the presence of oxygen and nitrogen atoms in the molecules) and hydrophobic interactions.

Phyo et al. [17] carried out enantioseparations using thirty-one chiral xanthonic derivatives on four macrocyclic antibiotic CSP (Chirobiotic V (vacomycin), Chirobiotic T (teicoplanin), Chirobiotic TAG (teicoplanin aglycone) and Chirobiotic R (ristocetin)) in different elution modes and performed docking studies to understand the underlying recognition mechanisms. The elution sequence calculated from the docking energies showed an agreement with the experimental results of 52%, 50%, 47% and 80% for Chirobiotic T, R, V and TAG columns, respectively. The prediction of elution sequences was not as expected, which might be due to

the relatively large diversity in types (steric, hydrophobic, hydrogen-bonding, ionic and π-π interactions) and numbers of interactions between the enantiomers and chiral selectors.

Papp et al. [58] determined the elution sequence of the pantoprazole enantiomers on a teicoplanin aglycon-based CSP in RPLC mode using a circular dichroism (CD) detector and performed molecular docking studies (*Figure 5*). Two types of interactions could be identified: hydrogen-bond and π-π interactions. In the docking poses, a high number of such interactions was identified for (R)-pantoprazole, in agreement with its stronger predicted binding affinity as well as the experimental elution sequence.

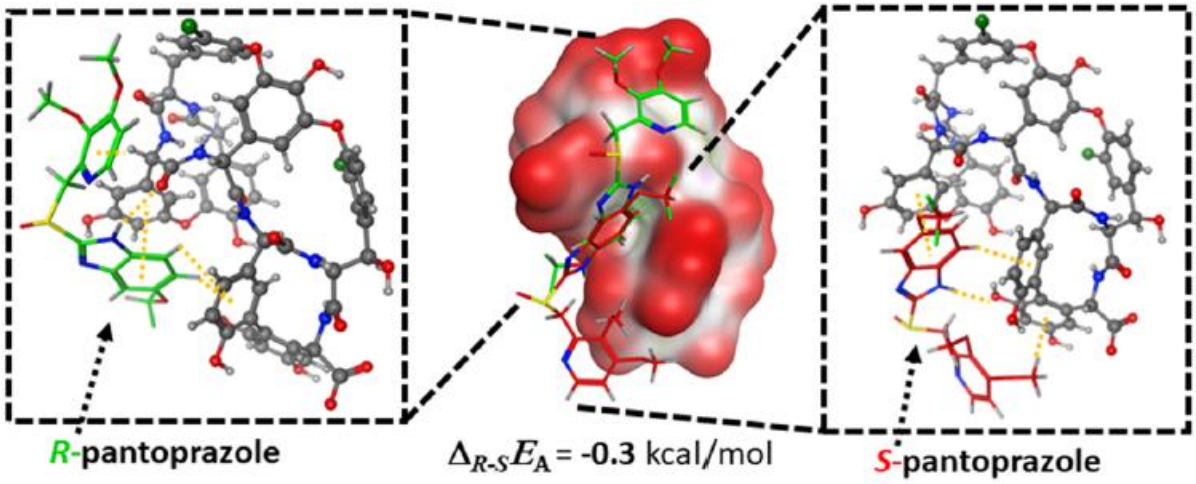

Figure 5. Docking calculations of pantoprazole enantiomers on teicoplanin aglycone CSP. The difference in binding energy between both enantiomers ($\Delta_{R\text{-}S}E_A$, calculated as the difference in binding energy between the R -and S enantiomer) is caused by the difference in the number of interactions between both enantiomers. Reproduced with permission from [58].

Shahnani et al. [59] studied the interactions between a vancomycin CSP and mandelic acid enantiomers in NPLC mode. The predicted binding energy was higher for the R enantiomer, and in agreement with its longer experimental retention time. The docking suggested that both enantiomers showed π-π and hydrogen-bond interactions with the vancomycin selector, but the R enantiomer interacts also similarly within the hydrophobic pockets of the selector. This

result confirmed the longer retention of the R enantiomer observed from the experimental results.

Cai et al. [60] performed molecular docking calculations of eight chiral psychoactive drugs (mirtazapine, sulpiride, promethazine, citalopram, oxazepam, cyamemazine, donepezil and oxybutynin) on a cellulose tris-(4-methylbenzoate) selector. For each pair of enantiomers, the difference between the binding energies ($\Delta\Delta E$) was calculated. The results were consistent with the experimental values for the enantioselectivity α. For example, out of this series of analytes, cyamemazine showed both the highest $\Delta\Delta E$ value and the largest difference in retention between both enantiomers. The docking pose in *Figure 6* clearly shows that both enantiomers are bound to the CSP in different orientations. For (S)-cyamemazine, π-π and hydrophobic interactions can be observed, whereas only hydrophobic interactions are for (R)-cyamemazine. This observation was used to explain the high $\Delta\Delta E$ value.
More generally spoken, the main interactions between the psychoactive enantiomers and CSP were hydrogen-bond, π-π and hydrophobic interactions [60].

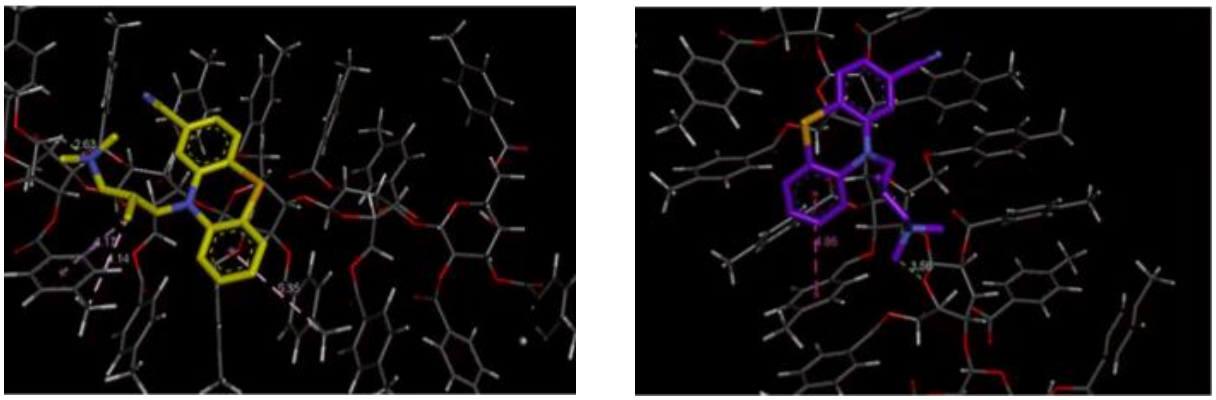

Figure 6. Docking calculations of cyamemazine enantiomers on cellulose tris-(4-methylbenzoate) CSP: (R)-cyamemazine is yellow and (S)-cyamemazine is purple. Reproduced with permission from [60].

Although high performance liquid chromatography (HPLC) is an important technique for chiral separations, SFC has recently gained popularity, among others of its shorter elution times. The latter are due to the low viscosity and high diffusivity of the supercritical fluid, which enables

using higher flow rates. As a consequence, it is a technique that has been extensively used in the pharmaceutical industry [56].

Zhao et al. [56] performed the enantioseparation of the pesticide napropamide by SFC using three polysaccharide CSP's (ADMPC, CDMPC and CCMPC) as well as docking calculations. (S)-napropamide eluted first on the amylose-based CSP, while (R)-napropamide did on the cellulose-based CSP. This was in accordance with the docking calculations, where hydrogen-bond interactions seem to be the most important for enantioseparation.

3. Fitting procedures

Fitting procedures try to make a correlation between the molecular structure expressed by using molecular descriptors and physical, chemical or biological properties in a regression model [28]. Since more than one hundred of CSP are available, method development for enantioseparations is challenging, because many chromatographic systems are possible and prediction of enantioselectivity not evident. As a consequence, molecules have to be analyzed by trial-and-error and screening approaches, which are labour intensive and time consuming [61]. A database named Chirbase, developed by Roussel and co-workers in the late 1980s [62], was an innovation to overcome this situation. Chirbase is a database containing data about enantioseparations and the applied conditions. This data can be used to build models to predict enantioseparation or to calculate descriptors, which can be also implemented into models. Although, Sheridan and co-workers [63] built models based on data from Chirbase, they concluded that it was difficult to obtain effective models. The main reason was that Chirbase contains only separation data for a limited set of molecules on a limited set of CSP, which means that not every molecule is tested on every CSP. This makes it difficult to build models for all possible CSP.

Models can be built to predict chromatographic retention of compounds. They can be divided in two groups: (i) models that describe retention of molecules under changing chromatographic

conditions, and (ii) models built for one chromatographic system to predict the retention of new molecules [61].

The first group of models are based on the retention prediction of a solute at given chromatographic conditions from a model derived on previous measurements for the same solute performed under varying chromatographic conditions. These models are generally based on the linear solvent strength model, which uses, for instance, for non-chiral RPLC the equation:

$$\log k = \log k_w - S\varphi \quad (1)$$

where k is the solute retention factor, $\log k_w$ is $\log k$ extrapolated to a mobile phase containing 0% of organic modifier, S is a constant for a compound in a certain chromatographic system and φ is the fraction of organic modifier present in the mobile phase [61].

The second group of models describes the relationship between a set of molecular descriptors and retention. They are called quantitative structure-retention relationships (QSRR). These relationships will be discussed further. An example of QSRR models are the linear free-energy relationships (LFER), also called linear solvation energy relationships (LSER) when used in HPLC to predict retention [61].

QSRR models can be built using chemometric tools, like multiple linear regression (MLR), partial least squares regression (PLS) and artificial neural networks (ANN). These models predict retention for new compounds, but also provide more information about the separation mechanism, identification of the most informative descriptors, evaluation of biological activities and of non-chromatographic properties [61].

These models are not always capable of distinguishing between enantiomers, because they use achiral molecular descriptors. Therefore chiral descriptors should be used to create models that can make a distinction between two enantiomers. In the next part of this review, the most important molecular descriptors that distinguish between enantiomers will be discussed. Then the modelling approaches are discussed to get insight in the most recent findings about predictive modelling.

3.1 Descriptors

QSRR models can be built to model and predict retention. As already stated above LSER use the Abraham descriptors, i.e. five descriptors to model a solute property (*SP*), for example, log *k* [8]. The equation is as follows:

$$SP = c + eE + sS + aA + bB + vV \quad (2)$$

The capital letters represent the solute descriptors, which are related to structural features. *E* is the excess molar refraction, *S* the solvatochromatic parameter π* (a combination of the polarity and the polarizability of the compound of interest *as a bulk sovent*), *A* and *B* the overall hydrogen-bond acidity (donating groups) and basicity (accepting groups), respectively, and *V* the McGowan characteristic volume. The lowercase letters are the system constants (model coefficients), related to the complementary effect of the stationary and mobile phase on these interactions, and *c* is the intercept of this equation [8]. For more information about LSER, we refer to ref. [64].

In QSRR approaches, molecular descriptors in general, calculated from the molecular formula or structure, may be used. For this purpose, software was developed, for example alvaDesc (Kode chemoinformatics srl., Pisa, Italy), BlueDesc (G. Hinselmann, University of Tübingen, Germany, 2008) and Mordred [65], which are able to calculate many descriptors [61].

Unfortunately these descriptors generally cannot distinguish between enantiomers. Therefore attempts have been made to devise descriptors that distinguish between enantiomers, the so-called chiral descriptors [66]. QSRR that use chiral descriptors are also called quantitative structure enantioselective retention relationships (QSERR).

Several research groups have developed chiral descriptors. Since we will mainly focus on more recent chiral descriptors, we refer to a review by Del Rio [19] for information about earlier developments in this domain.

The group of West was the first to use LSER relationships to predict the degree of separation between two enantiomers (but not their elution sequence) [67]. The LSER model in this study was augmented with two additional descriptors, flexibility (*F*) and globularity (*G*), because these quantities are thought to be important in the chiral recognition mechanism.

Aires-de-Sousa and Gasteiger [68] developed the so-called chirality codes, which represent chirality using a fixed set of descriptors. This set offers a mathematical description of the stereochemical properties of a molecule and, crucially, distinguishes between enantiomers. The group of Caetano and co-workers [69] used the so-called conformation-dependent chirality codes (CDCC) to build models for a congeneric set of molecules in order to make predictions about the enantioselectivity on a teicoplanin and bianthracene-based CSP using classification and regression trees. The CDCC represent chirality by considering all possible combinations of 4 atoms in the molecule. For each such combination, the position vectors of the 4 atoms are mathematically combined in a specific order that depends on atomic properties. For this congeneric series of molecules, the elution sequence could be well predicted using these chirality codes, but these descriptors cannot be interpreted from a physicochemical point of view, which made it difficult to find reasons why certain molecules were misclassified.

Later on, Del Rio and Gasteiger [70] extended this approach, giving rise to the so-called chiral enantiophores. These can be inserted into structure chiral activity relationships (SCAR) to be related with the experimental elution sequence of enantiomers in HPLC separations, starting from information about the absolute configuration of enantiomers [70]. The idea behind this new type of descriptor is to calculate R- and S-like properties of atom combinations which are given at different bond distances from the stereogenic centre [70]. First, bond distances starting from the chiral centre are determined. An example of this methodology can be observed in *Figure 7*: the atoms next to the stereogenic centre receive number “1”. Atoms that are two bindings away from the chiral centre receive number “2”, and so on. Secondly, special atom types of the molecule are determined, which are atoms that exert specific interactions

with the chiral selector to achieve a chiral separation. These atom types, based on prioritization rules, discriminate whether an atom combination has to be used or not in the descriptor calculation. A fixed-length vector of 20 descriptors per molecule is obtained, which denotes the chirality of the enantiomers. When the retention of a new compound is predicted, it is possible to assign the absolute configuration to the elution sequence [70].

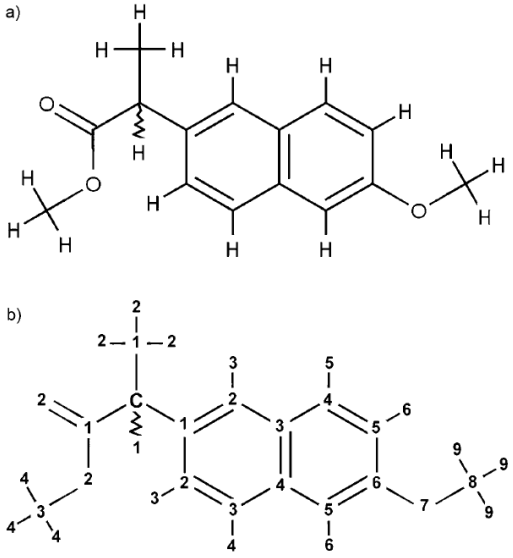

Figure 7. Example of a molecule (a) and its bond distances around the stereogenic centre “C” (b) [70].

Dervarics et al. [71] developed another type of descriptor, the so-called chirality-sensitive flexibility descriptor, where positions of 4 predefined pharmacophores in a predefined order are combined. While this class of descriptors received comparatively less attention, their physical interpretation is considerably more straightforward than previous work, because pharmacophores represent concrete physicochemical properties directly related to intermolecular interactions. The descriptor is based on pharmacophore points derived from endomorphin- and prostaglandin analogues. It led to QSAR models, which could make good predictions about the biological activity of endomorphin- and prostaglandin analogues.

In 2008, Marrero-Ponce et al. [72] developed new chiral descriptors to distinguish between non-chiral and chiral molecules, named “3D-chiral TOMOCOMD-CARDD” (topological molecular computer design – computer-aided rational drug design) descriptors. The same descriptors were later re-implemented in a more user-friendly cross-platform Java application

named QuBiLS-MAS (Quadratic, Bilinear and N-Linear mapS based on graph-theoretic electronic-density Matrices and Atomic weightingS) [73]. The TOMOCOMD-CARDD molecular descriptors encode the structure of a molecule by means of linear, bilinear and quadratic transformations. Therefore they calculate an atom-based molecular vector and the so-called non-stochastic and stochastic graph-theoretic electronic-density matrices. The calculations lead to several atom- and bond-based TOMOCOMD-CARDD molecular descriptors, which can be used to build models. The theory about these descriptors is discussed more in detail in reference [74].

These descriptors do not give information about the 3D structure of the molecule. Consequently, a trigonometric 3D-chirality correction factor was introduced in the molecular vector to give some stereochemical information. This factor can take three values: 1, 0 and -1 for R, achiral and S atoms respectively [74]. On 3 QSAR test sets, these molecular descriptors proved competitive with previously reported chiral topological indices [74].

3.2 Multivariate modelling

As already mentioned, different modelling techniques can be used to model the relationship between a dependent variable, for example, retention, and a set of independent variables, the molecular descriptors. The purpose of these models is to make predictions about new compounds by calculating their molecular descriptors and introducing them into the model.

Actually two types of models do exist: global and local models. Global models split the data set into a training and test set (on the condition that the data set is large enough). The model is built with the compounds that belong to the training set, while the model is validated with the test set. Local models divide the data set in groups, for example acid, basic and neutral compounds and these groups are separately further divided into training and test sets (when large enough). The data may also be split based on similarities in these molecular descriptors. In general this will give a smaller prediction error than global models [66].

To build models, regression methods may be necessary and several of these methods do exist.

MLR is a regression method to build a linear relationship between a dependent variable, e.g. retention, and predictor variables, e.g. molecular descriptors. In first instance the variables have to be normalized or standardized, after which the MLR model can be build. The advantage of such model is that each coefficient linked to a descriptor gives information about its importance and influence on the response. The importance of the descriptors can be interpreted physicochemically. Therefore MLR is the most applied method when information is needed about the separation mechanism [66].
On the other hand, modelling techniques like PLS and ANN can be better predictive and handle some non-linearity and collinearity between the descriptors, whereas MLR cannot [66].

Before building a model, data pretreatment has to be performed. In first instance the number of predictor variables (descriptors) have to be reduced. This can be executed by (1) removing the variables that are highly correlated to each other, because they provide the same information, and (2) removing the variables that are rather constant, because they do not have any influence on the dependent variable. Subsequently the variables should be normalized or standardized in order to have a meaningful model. Furthermore the number of descriptors included in the model should be low. Therefore variable selection is often combined with the modelling approach, e.g. genetic algorithms (GA), stepwise regression,… [61, 75].

In the following paragraphs of this review some modelling approaches are discussed.

Table 3. Some recent modelling approaches. *The retention factor (*k*) can be defined as the time a compound resides on the stationary phase relative to its time in the mobile phase. ** The selectivity (α) is a measure of the distance between the maxima of two peaks. A higher selectivity means that the peak maxima are further away from each other (α = 1 means that both peaks have the same retention time) [76]. In case of chiral separations, α is also called the enantioselectivity.

Dataset	CSP[(1)] (separation method)	Approach	Descriptors/ modelling technique	Predicted values	Year (reference)
130.000 solutes from Chirbase	19 CSP (HPLC)	QSAR	AP, DP and MOE_2D / random forest (RF)	*α* ** and log *α*	2016 [63]
171 achiral analytes and 97 racemates	ADMPC, CDCPC, CDMPC (HPLC & SFC)	QSRR (LSER)	Abraham descriptors/ MLR	Log *k* *	2016 [8]
26 ethanol ester enantiomers	CDMPC (HPLC)	QSRR	Molecular, quatum mechanical and multivariate image analysis (MIA) descriptors / MLR, PLS, PCR	Retention times	2017 [75]
134.000 solutes from Chirbase	41 CSP (HPLC)	QSAR	RDKit layer fingerprints / RF	*α*	2018 [77]
16 racemic coumarin derivatives	ADMPC, amylose tris-(5-chloro-2-methylphenyl-carbamate) (HPLC)	QSPR	Descriptors corresponding to properties of substituents on phenyl rings / MLR	Log *k* and log *α*	2018 [54]
34 compounds (basic drugs and pesticides)	CDCPC (HPLC)	QSPR	Structural variables / DPLS1	Categorical enantio-resolution	2018 [78]
145 achiral analytes and 67 racemates	Chirobiotic T, TAG and V2 (SFC)	QSRR (LSER)	Abraham descriptors/ MLR	Log *k*	2019 [79]

50 arylhydantoin compounds	Whelk-O1 (HPLC)	QSPR	Molecular parameters derived from VolSurf / PLS	Log *k* and log *α*	2020 [80]
53 chiral compounds	ADMPC, amylose tris-(5-chloro-2-methylphenyl-carbamate), ACMPC (HPLC)	QSPR	Structural variables / DPLS1	Categorical enantio-resolution	2020 [94]

(1) ACMPC: amylose tris-(3-chloro-5-methylphenylcarbamate)

In the past, regression methods have been applied to describe relationships between retention and molecular descriptors. Examples can be found in Booth et al. [81, 82], Montanari et al. [83] and in [69, 84, 85, 86].

More recently, the random forest (RF) method is also used [63, 77]. If an RF approach is applied, several decision trees are created. Depending on the data two types of trees exist: when the response is categorical, a classification tree is obtained and when the response is continuous, a regression tree. Building trees is based on a binary recursive splitting procedure, which divides the data set into two subsets and the process is then repeated for every subset. First, a root node is built, containing all objects of the dataset. This root node is split into two child nodes, which are more homogeneous than the parent node. The split criterion can be any value of any variable in the descriptor set. For every child node the splitting can continue until a terminal node is reached, which is sufficiently homogeneous or contains only one element. A child node that splits into two other child nodes, is named a parent node [69]. The structure of such a tree is illustrated in *Figure 8*. An RF consists of several decision trees and can be created as follows: consider a number of n trees [T_1 (X),…, T_n (X)], where x is a vector of molecular descriptors. The entire number of trees produces n outputs [$\hat{Y}_1 = T_1(X)$,…, $\hat{Y}_n = T_n(X)$], with $\hat{Y}_n$ the prediction for a molecule by the *n*th tree. The outputs of all trees generate one final prediction, $\hat{Y}$. In case of regression trees $\hat{Y}$ is the average of the individual tree

predictions, while in case of classification trees, $\hat{Y}$ is the class predicted by the majority of trees [87]. More information about the RF methodology can be found in reference [87].

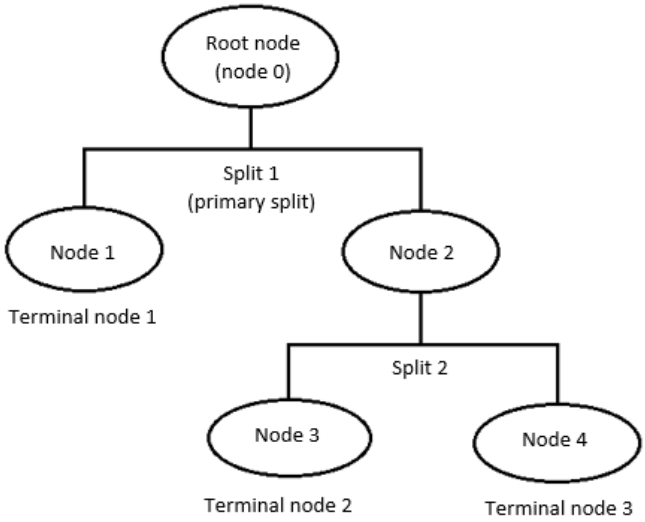

Figure 8. Structure of a classification or regression tree. Node 0 is the root node containing all objects. Node 2 is a parent node, which is split into two child nodes. Nodes 1, 3 and 4 are terminal nodes.

Sheridan et al. [63] used RF to build quantitative structure activity relationships (QSAR) for the prediction of chromatographic enantioselectivity on different polysaccharide and macrocyclic antibiotic CSP based on HPLC data from Chirbase. These QSAR models, when built and validated properly, allow predicting enantioselectivity based on certain structural features and properties, without the need to understand the underlying mechanism. The scope of this model was to predict the separation factor *α* for enantiomers resolved on different CSP, including some polysaccharide and macrocyclic antibiotic CSP. The topological descriptors used in this model, dubbed AP, DP and MOE_2D, are briefly explained in the next paragraph.

AP, the Carhart atom pair, is of the form “atomtype 1 – (distance) – atomtype 2”, where “atom type” contains element type, number of π-electrons and number of non-hydrogen neighbours, and “distance” signifies the distance in bonds between the two atoms [63, 88]. DP is similar to AP, but the atomtype is defined differently. The atoms are assigned to one of seven binding property classes: cations, anions, neutral hydrogen-bond donors, neutral hydrogen-bond acceptors, polar atoms, hydrophobic atoms and other [63, 89]. The authors briefly state that

they explored “alternative versions of AP and DP that take stereochemistry into consideration”; it is further implied that the atom types are augmented with an R/S and/or chiral/nonchiral classification. Molecular Operating Environment_2D (MOE_2D) contains 186 achiral molecular descriptors generated by the MOE software [63, 90].

An RF regression approach was applied, but only for 4 out of 19 CSP an acceptable QSAR model could be built. According to the authors, the reason was the lack of good data in Chirbase. Some molecules were not tested on different CSP in certain conditions, which makes it rather difficult to take conclusions about enantioseparations, because on other CSP a separation might be obtained. Another problem was that only a small number of unsuccessful experiments is included, which leads to an imbalanced distribution of the data [63, 77].

In a next study [77], the same authors attempted to improve the predictivity of their RF classifier approach by tackling the problem of the imbalanced data distribution. The data was divided into 4 classes based on enantioselectivity, i.e. class 1: no or poor separation ($1 \leq \alpha < 1.10$); class 2: separation is achieved or almost ($1.10 \leq \alpha < 1.20$); class 3: excellent separation ($1.20 \leq \alpha < 2.10$) and class 4: large separation ($\alpha \geq 2.10$). The prediction rates improved, but the accuracies seemed to vary considerably within each class. This might still be due to the imbalanced class distribution, because classes 1, 2, 3 and 4 contain 10-15, 20-30, 45-55 and 10-15% of the data sets, respectively. In order to provide balanced data sets and to increase the predictive ability, a two-step approach had to be performed: the first step consists of over-sampling the two minority classes (class 1 and 4) and down-sampling the two majority classes (classes 2 and 3). In a second step, the classes were aggregated to two: none-to-moderate enantioselectivity (classes 1 and 2) and high enantioselectivity (classes 3 and 4). The results now showed a good predictivity for 34 out of 41 CSP.

In a study by Pisani et al. [54], QSPR models were built by MLR to investigate the enantiorecognition mechanism of several racemic 7-[1-alkylpiperidin-3-yl)methoxy]coumarin derivatives on an ADMPC CSP in polar organic solvents chromatography (POSC) mode. The following descriptors, from which none seems to be chiral, were used in their models: (1)

Hammett sigma constant, which accounts for the effect of aromatic substituents in the molecule on the electronic interactions, such as dipole-dipole and π-π interactions, with the aromatic substituents on the CSP; (2) Molar refractivity and (3) van der Waals volume, which both account for steric fitting of the aromatic substituents into the CSP; (4) Hansch lipophilic constant for the aromatic substituents and (5) fragment lipophilic value calculated from log k_w (with k_w the retention factor extrapolated to 100% aqueous mobile phase).

Two models were built with log *k* as response: one for the first eluted and one for the last eluted enantiomers. Considering the first-eluted enantiomer model, the most important descriptor seems to be the Hammett sigma constant (positive effect). As a consequence, the retention of the first enantiomers might be mostly determined by π-π interactions. Eventually, a model for the logarithm of the enantioselectivity (log α) was obtained, containing 2 descriptors: van der Waals volume (negative coefficient), indicating the importance of steric properties and an indicator variable (positive coefficient), which takes the value 1 for meta-substituted and 0 for para-substituted compounds.

Other groups were also important for hydrogen-bond interactions with the CSP, as seen in the docking simulations described above. In addition, the size of the substituents and their position (meta position is better than para) are of high importance in the retention of those compounds on the ADMPC CSP.

Luo et al. [80] developed QSPR models to predict the retention and separation factor of 50 arylhydantoin compounds. The descriptors in their PLS regression models were derived from the molecular interaction fields (MIF) computed by the GRID software, a computational tool to map molecular surfaces of molecules [91, 92]. Specifically, the VolSurf software was used to analyze the MIF by adding probes (mostly water and a hydrophobic probe) and computes the volume and surface of regions where the interaction energy values are below certain cut-off limits. As a result, conformation-dependent parameters are obtained describing the distribution of hydrophobic and hydrophilic regions around the molecule [92].

Two models were built for the retention factor (log *k*): one for the more retained enantiomers and one for the less retained. The model considering the more retained enantiomers (using 6 latent variables) showed a leave-one-out cross-validation determination coefficient (q^2_{LOO}), a parameter for the predictive ability of the model, of 0.884, while the other model (using 7 latent variables) showed a q^2_{LOO} of 0.885. This means that models built show a good predictive ability for retention. When both models were compared, the descriptors important for the hydrophobic interactions show an opposite correlation with the retention factor. This could be observed after plotting the PLS coefficients against the descriptors.

Two other PLS models were built for the logarithm of the separation factor (log *α*): one for the entire data set and one after splitting the data in a training set of 38 compounds and a test set of the remaining 12 compounds, in order to test the predictive ability. Using 38 latent variables, the first model showed a q^2_{LOO} of 0.805 and for the second model, a q^2_{LOO} of 0.802 was obtained. The models appeared to show a good predictive ability and were claimed to predict even the elution sequence very well.

Barfeii et al. [75] made a QSRR approach to predict the retention times of 26 ethanol ester enantiomers on a CDMPC CSP in HPLC by using different types of descriptors: structural descriptors, electronic and quantum mechanical descriptors and multivariate image analysis (MIA) descriptors. MIA descriptors are calculated by transforming two-dimensional images of a molecular structure into pixels. Since different structures lead to different pixel coordinates, MIA can be used to explain the variance in retention times of molecules and can even make a difference between two enantiomers.

In addition, different modelling techniques were investigated to determine which one provides the best predictions. The used techniques are MLR, PLS and principal component regression (PCR). The best predictions were obtained with PLS in combination with MIA and structural descriptors. These models showed a high correlation between the modelled variables and the observed retention times, a low root mean square error (RMSE) and a high q^2_{LOO}.

The previous studies [54, 75, 80] were carried out for structurally related compounds. As a consequence information was obtained about the functional groups responsible for the enantioseparation, considering certain compounds and its derivatives [78]. Actually these models can only predict properly for compounds which are structurally related to the data set used to build and validate these models. However, some other research groups have built models using a structurally diverse set of molecules and this is discussed in the following part of this review.

A set of 34 structurally unrelated chiral compounds (pesticides and basic drugs) were used by Martín-Biosca et al. [78] to construct a model predicting the enantioresolution as a categorical variable (R_sC) as a function of 58 structural variables, such as chiral topological parameters, e.g. *C** (counts for atoms or groups bonded to the chiral carbon atom), molecular topological parameters (aromatic ring count) and octanol-water partition coefficient (log *P*). If $R_sC = 0$, no baseline separation is obtained and if $R_sC = 1$, baseline separation is observed under the given conditions. These categorical enantioresolution levels were established from experimental resolution values in RPLC on a CDCPC CSP. The structural variables were linked to the R_sC using discriminant partial least squares for one categorical response variable (DPLS1). The initial model provided full discrimination between separated and non-separated compounds for the calibration set, but some misclassifications occurred in the cross-validated output. As a consequence the predictive power of this model was poor. The regression coefficients indicate also that most of the variables were non-significant, except the variables *C*hA* (distance between chiral carbon atom and aromatic heterocycles), log *D* (apparent log *P* at a given pH) and molar total charge.

A model refinement was carried out, eliminating variables one by one until the elimination of more variables worsen the quality (predictive power) of the model. Nine descriptors were used in this model: two chiral topological parameters (*C*X* the distance between chiral carbon atom and heteroatoms and *C*hA*), a molecular topological parameter (aromatic ring count *Arc*) and six other molecular descriptors (minimal z length (*zmin*), molecular surface area (*MSA*), orbital

electronegativity of the chiral carbon atom (*OEC**), surface tension (*ST*), log*D* and molar total charge). The molar total charge contributes (negatively) the most to enantioresolution. As a consequence, neutral and low charged compounds show the largest probability of enantioresolution. The contribution of the other variables on the enantioseparation is almost equivalent. The enantioresolution improved when heteroatoms or aromatic heterocycles directly linked to the chiral carbon atom are absent (*C*X* and *C*hA* coefficients are negative) and when aromatic groups are present in the molecule (*Arc* coefficient is positive).

Finally, an explicit model was derived by DPLS1 to anticipate whether a new compound will be resolved or not. A model was built with "*eRs*" as response, which is an indicative value for the resolution (*Rs*). To anticipate resolution, these *eRs* outputs have to be transformed into anticipated *RsC* (*aRsC*) outputs. If *eRs* > 0.5, baseline separation is obtained (*aRsC* = 1); 0.4 < *eRs* < 0.5 means almost baseline separation (*aRsC* = 0.5); and *eRs* < 0.4 means poor or no enantioseparation (*aRsC* = 0). This model provided 100% of correct anticipations for a test set of 4 compounds when comparing these *aRsC* values to *RsC* values from experimental data.

In a more recent study [93] this group performed a modelling study of R_sC with DPLS1 using 53 structurally unrelated compounds on three amylose-based CSP: ADMPC, amylose tris-(5-chloro-2-methylphenylcarbamate) and ACMPC. The experiments were carried out in RPLC mode and only ADMPC and ACMPC results were used to build the models, because amylose tris-(5-chloro-2-methylphenylcarbamate) showed less good separations. Fifty-eight structural variables were used to build the models, such as chiral topological parameters, molecular topological parameters (aromatic bond count (*Abc*), ring count (*Rc*)), the count of atoms or groups in the entire molecule and other descriptors (e.g. hydrogen-bonding acceptor (*HBA*), hydrogen-bonding donor (*HBD*), log *P*).

Considering ADMPC, the variables favouring enantioseparation are three chiral topological parameters (*C*C=O* (distance between chiral carbon and a carbonyl group), *C*X* and *C*H*). The presence of a carbonyl function is important for enantioseparation, because it may act as hydrogen-bond acceptor and be important for π-π interactions. Additionally, the absence of heteroatoms (*C*X*) and hydrogen atoms (*C*H*) linked to the chiral carbon atom, the absence

of aliphatic bonds in the molecule (*abc* and *bc* variables) and the presence of a ternary amine (hydrogen-bond acceptor) favours enantioresolution as well.

Considering ACMPC, it was observed that the chiral topological parameter *C*C=O* favours enantioresolution, because carbonyl groups are important for hydrogen-bond interactions and π-π interactions. The presence of aromatic bonds and fused rings (*Abc* and *frc* variable respectively) favours also enantioresolution as well as the presence of nitrogen in aromatic rings (*NA* variable), which was opposite to ADMPC. They are important for hydrogen-bond and π-π interactions, but on ACMPC, the formation of a Lewis adduct between the aromatic amines (Lewis base) and the chlorine atom on the phenylcarbamate (Lewis acid) and/or between the aromatic amines and the acidic proton on the carbamate group of the CSP occur also.

The model constructed for ADMPC has a better predictive ability, but is more complex. It contains 7 latent variables, whereas the ACMPC model only 2.

Enantioselective HPLC is the preferred technique to perform chiral separations, but as already stated SFC becomes more important nowadays. Consequently, modelling approaches were also applied for this technique.

For instance, Khater et al. [8] compared NPLC and SFC on polysaccharide CSP by building QSRR and discriminant analysis (DA) models. For the QSRR models, the Abraham descriptors were used besides two additional descriptors, named flexibility (*F*) and globularity (*G*), which are important properties for enantioselective chromatography [94], [95]. Such LSER-derived models were already used earlier to study the chiral recognition mechanism on polysaccharide and macrocyclic antibiotic CSP, both in HPLC and SFC [67, 94, 96, 97, 98]. The equation can be described as follows (with *F* and *G* the additional descriptors):

$$\log k = c + eE + sS + aA + bB + vV + fF + gG \qquad (3)$$

A difference in interactions between NPLC and SFC was observed. The interactions with π and n electrons (*e* coefficient) and proton donors (*a* coefficient) were stronger in SFC, whereas

the interactions with dipoles (*s* coefficient) and proton acceptors (*b* coefficient) were stronger in NPLC. This may be caused by the fact that (1) CO_2 has more possibilities for polar interactions than heptane, the solvent used in the NPLC mobile phases, because CO_2 is more polarizable. (2) CO_2 and alcohol mixtures are heterogeneous (the amount of alcohol present in the mobile phase is low), with alcohol molecules clustering around analytes, leading to stronger hydrogen-bonding and dipole-dipole interactions with the mobile phase.

The coefficients related to size (*v*) and shape (*g*) have opposite signs in the SFC and NPLC models. The retention seems to increase in SFC when the hydrocarbon volume increases (positive *v* coefficient), while this decreased the retention in NPLC [8].

In a next step the enantioselectivity between SFC and NPLC was compared by performing DA, which was applied to help understanding which structural features are involved in the resolved racemates. DA on the complete dataset from polysaccharide CSP did not perform well, because analytes may enter different interaction sites on the CSP, due to the presence of different chiral cavities on these CSP. Therefore, two classes may be defined in two different approaches, either co-eluting and (partly) resolved racemates, and fast eluting versus late eluting racemates. In a first approach, the latter distinction is made by the authors based on the expected retention (estimated from earlier built QSRR models for the same CSP, compared with the experimental retention): one set of racemates eluting earlier than expected and those eluting later than expected. Differences between experimental and predicted retention indicate rather a lack of fit of the model applied. Therefore it seems strange to define classes based on this criterion.

DA analysis allows considering the contributions of the considered descriptors in both SFC and NPLC and to compare both in order to relate this to retention and enantioselectivity.

In a second DA, a distinction was made between separated and non-separated racemates within the early or late eluting compounds. This was done to evidence the structural features of separated racemates, to study differences appearing between the NPLC and SFC, as well as to observe different enantioselective interactions [8].

Khater et al. [79] built LSER models to study the retention and enantiorecognition mechanisms in SFC on three macrocyclic antibiotic CSP. Two additional descriptors were added to the five standard Abraham descriptors, named D^- and D^+, to take ionic interactions into account. For the three CSP, the same pattern of interaction was observed: positive *e*, *s*, *a*, *b* and d^+ coefficients and negative *v* and d^- coefficients. The most important interactions are hydrogen-bond interactions (*a* and *b* coefficients), because of the presence of peptide, phenolic and hydroxyl functions on the CSP. Hydrogen-bonding with proton donor analytes was larger on the vancomycin phase than on the teicoplanin phases, which means that the retention of these analytes might be stronger on a vancomycin CSP. On the other hand, the hydrogen-bonding with proton acceptor analytes was lower on the vancomycin CSP. The *e* -and *s* coefficients were also positive, resulting from π-π interactions (between aromatic groups) and dipole-dipole interactions, respectively. These interactions were less significant than hydrogen-bonding, because lower coefficients were obtained. Since the d^- coefficient is negative and d^+ is positive, the anionic acid functions of the CSP can easily interact with the analytes. As a consequence, cations are longer retained, whereas anions are not. The d^+ coefficient on the vancomycin CSP is significantly lower than on the teicoplanin CSP, because vancomycin may contain a free amine function. This leads to more repulsion of cations, but since the d^- coefficient is almost the same as on the other CSP, there is no favourable interaction with anions.

4. Conclusions

Polysaccharide- and macrocyclic antibiotics-based chiral selectors are very popular for chiral separations. Many efforts have already been made to elucidate their chiral recognition mechanisms. In recent decades, computer models contributed significantly to these efforts. Atomistic docking calculations and molecular dynamics simulations as well as empirical modelling have been employed to this end, and yielded a number of important insights.

Owing to their ease of operation and computational efficiency, molecular docking calculations have long been a mainstay for studying the interactions between CSP and enantiomers, and are presently still a popular choice for this purpose. However, they generally use energy functions that were optimized for protein receptors in an aqueous medium. As a consequence, these methods can be expected to be less accurate for polysaccharide and macrocyclic antibiotic chiral selectors in mobile phases that typically differ significantly from pure water. Moreover, an inherent drawback of docking calculations is that they are traditionally static. While recent software allows for flexible treatment of a small selection of receptor side chains, this comes at a significant computational cost. Explicit solvent molecular dynamics simulations, on the other hand, take the solvent effect and the dynamic process of enantiorecognition during chromatographic separations into account. Historically, this was extremely time-consuming, but because of computational progress, the use of these methods has become somewhat common.

Besides these atomistic calculations, empirical modelling studies have been performed as well, in order to develop models with good predictive abilities. These models should be built with chiral descriptors in order to distinguish between enantiomers. However, there is still a lack of universally advantageous chiral descriptors. On the one hand, descriptors such as the chirality codes and chiral enantiophores have been shown to yield good predictions on a number of test sets, but cannot be interpreted from a physicochemical point of view, which makes it difficult to understand the underlying mechanisms. The so-called chirality-sensitive flexibility descriptor, on the other hand, is a chiral descriptor that can be interpreted physicochemically, because it is based on pharmacophore points derived from a molecular structure. Unfortunately it is not trivial to apply this type of descriptor to a diverse set of molecules. In summary, notwithstanding the existence of some chiral descriptors, research to develop suitable descriptors, which allow building suitable models that enable accurate predictions for diverse molecules and separation conditions, is therefore still necessary.

References

[1] B. Zhao, P.A. Oroskar, X. Wang, D. House, A. Oroskar, A. Oroskar, C. Jameson, S. Murad, The composition of the mobile phase affects the dynamic chiral recognition of drug molecules by the chiral stationary phase, Langmuir 33 (2017) 11246-11256.

[2] X. Wang, C.J. Jameson, S. Murad, Modeling enantiomeric separations as an interfacial process using amylose tris (3,5-dimethylphenyl carbamate)(ADMPC) polymers coated on amorphous silica, Langmuir 36 (2020) 1113-1124.

[3] B.S. Sekhon, Exploiting the power of stereochemistry in drugs: an overview of racemic and enantiopure drugs, J. Mod. Med. Chem. 1 (2013) 10-36.

[4] FDA'S policy statement for the development of new stereoisomeric drugs, Chirality 4 (1992) 338-340.

[5] E.R. Francotte, Enantioselective chromatography as a powerful alternative for the preparation of drug enantiomers, J. Chromatogr. A 906 (2001) 379-397.

[6] M. Lämmerhofer, Chiral recognition by enantioselective liquid chromatography: mechanisms and modern chiral stationary phases, J. Chromatogr. A 1217 (2010) 814-856.

[7] D. Speybrouck, E. Lipka, Preparative supercritical fluid chromatography: A powerful tool for chiral separations, J. Chromatogr. A 1467 (2016) 33-55.

[8] S. Khater, M.A. Lozac'h, I. Adam, E. Francotte, C. West, Comparison of liquid and supercritical fluid chromatography mobile phases for enantioselective separations on polysaccharide stationary phases, J. Chromatogr. A 1467 (2016) 463-472.

[9] Y. Okamoto, R. Aburatani, K. Hatada, Chromatographic chiral resolution: XIV. Cellulose tribenzoate derivatives as chiral stationary phases for high-performance liquid chromatography, J. Chromatogr. A 389 (1987) 95-102.

[10] Y. Okamoto, R. Aburatani, S.I. Miura, K. Hatada, Chiral Stationary Phases for HPLC: Cellulose Tris (3,5-dimethylphenylcarbamate) and Tris (3,5-dichlorophenylcarbamate) Chemically Bonded to Silica Gel∗, J. Liq. Chromatogr. Relat. Technol. 10 (1987) 1613-1628.

[11] Y. Okamoto, R. Aburatani, T. Fukumoto, K. Hatada, Useful chiral stationary phases for HPLC. Amylose tris (3,5-dimethylphenylcarbamate) and tris (3,5-dichlorophenylcarbamate) supported on silica gel, Chem. Lett. 16 (1987) 1857-1860.

[12] D.W. Armstrong, Y. Tang, S. Chen, Y. Zhou, C. Bagwill, J.R. Chen, Macrocyclic antibiotics as a new class of chiral selectors for liquid chromatography, Anal. Chem. 66 (1994) 1473-1484.

[13] P. Peluso, A. Dessì, R. Dallocchio, V. Mamane, S. Cossu, Recent studies of docking and molecular dynamics simulation for liquid-phase enantioseparations, Electrophoresis 40 (2019) 1881-1896.

[14] Y. Okamoto, E. Yashima, Polysaccharide derivatives for chromatographic separation of enantiomers, Angew. Chem. Int. Ed. 37 (1998) 1020-1043.

[15] J.M. Padró, S. Keunchkarian, State-of-the-art and recent developments of immobilized polysaccharide-based chiral stationary phases for enantioseparations by high-performance liquid chromatography (2013–2017), Microchem. J. 140 (2018) 142-157.

[16] J. Shen, T. Ikai, Y. Okamoto, Synthesis and application of immobilized polysaccharide-based chiral stationary phases for enantioseparation by high-performance liquid chromatography, J. Chromatogr. A 1363 (2014) 51-61.

[17] Y. Phyo, S. Cravo, A. Palmeira, M.E. Tiritan, A. Kijjoa, M.M. Pinto, C. Fernandes, Enantiomeric resolution and docking studies of chiral xanthonic derivatives on chirobiotic columns, Molecules 23 (2018) 142.

[18] A. Berthod, Chiral recognition mechanisms with macrocyclic glycopeptide selectors, Chirality 21 (2009) 167-175.

[19] A. Del Rio, Exploring enantioselective molecular recognition mechanisms with chemoinformatic techniques, J. Sep. Sci. 32 (2009) 1566-1584.

[20] G.K.E. Scriba, Chiral recognition in separation sciences. Part I: Polysaccharide and cyclodextrin selectors, Trends Anal. Chem. 120 (2019) 115639.

[21] P. Peluso, V. Mamane, R. Dallocchio, A. Dessì, S. Cossu, Noncovalent interactions in high-performance liquid chromatography enantioseparations on polysaccharide-based chiral selectors, J. Chromatogr. A 1623 (2020) 461202.

[22] P. Peluso, V. Mamane, S. Cossu, Liquid chromatography enantioseparations of halogenated compounds on polysaccharide-based chiral stationary phases: Role of halogen substituents in molecular recognition, Chirality 27 (2015) 667-684.

[23] P. Peluso, V. Mamane, E. Aubert, A. Dessì, R. Dallocchio, A. Dore, P. Pale, S. Cossu, Insights into halogen bond-driven enantioseparations, J. Chromatogr. A 1467 (2016) 228-238.

[24] P. Peluso, V. Mamane, R. Dallocchio, A. Dessì, R. Villano, D. Sanna, E. Aubert, P. Pale, S. Cossu, Polysaccharide-based chiral stationary phases as halogen bond acceptors: A novel strategy for detection of stereoselective σ-hole bonds in solution, J. Sep. Sci. 41 (2018) 1247-1256.

[25] P. Peluso, V. Mamane, A. Dessì, R. Dallocchio, E. Aubert, C. Gatti, D. Mangelings, S. Cossu, Halogen bond in separation science: A critical analysis across experimental and theoretical results, J. Chromatogr. A 1616 (2020) 460788.

[26] E. Yashima, C. Yamamoto, Y. Okamoto, NMR studies of chiral discrimination relevant to the liquid chromatographic enantioseparation by a cellulose phenylcarbamate derivative, J. Am. Chem. Soc. 118 (1996) 4036-4048.

[27] N.M. Maier, P. Franco, W. Lindner, Separation of enantiomers: needs, challenges, perspectives, J. Chromatogr. A 906 (2001) 3-33.

[28] K.B. Lipkowitz, Theoretical studies of type II–V chiral stationary phases, J. Chromatogr. A 694 (1995) 15-37.

[29] R. Sardella, E. Camaioni, A. Macchiarulo, A. Gioiello, M. Marinozzi, A. Carotti, Computational studies in enantioselective liquid chromatography: Forty years of evolution in docking- and molecular dynamics-based simulations, Trends Anal. Chem. 122 (2020) 115703.

[30] S.A. Hollingsworth, R.O. Dror, Molecular Dynamics Simulation for All, Neuron 99 (2018) 1129-1143.

[31] J.A. Izaguirre, S. Reich, R.D. Skeel, Longer time steps for molecular dynamics, J. Chem. Phys. 110 (1999) 9853-9864.

[32] J.D. Durrant, J.A. McCammon, Molecular dynamics simulations and drug discovery, BMC Biol. 9 (2011) 71.

[33] A. Hospital, J.R. Goñi, M. Orozco, J.L. Gelpí, Molecular dynamics simulations: advances and applications, Adv. Appl. Bioinform. Chem. 8 (2015) 37-47.

[34] K. Vanommeslaeghe, O. Guvench, A.D. Mackerell Jr, Molecular mechanics, Curr. Pharm. Des. 20 (2014) 3281-3292.

[35] D.A. Case, H.M. Aktulga, K. Belfon, I.Y. Ben-Shalom, S.R. Brozell, D.S. Cerutti, T.E. Cheatham, III, V.W.D. Cruzeiro, T.A. Darden, R.E. Duke, G. Giambasu, M.K. Gilson, H. Gohlke, A.W. Goetz, R. Harris, S. Izadi, S.A. Izmailov, C. Jin, K. Kasavajhala, M.C. Kaymak, E. King, A. Kovalenko, T. Kurtzman, T.S. Lee, S. LeGrand, P. Li, C. Lin, J. Liu, T. Luchko, R. Luo, M. Machado, V. Man, M. Manathunga, K.M. Merz, Y. Miao, O. Mikhailovskii, G. Monard, H. Nguyen, K.A. O'Hearn, A. Onufriev, F. Pan, S. Pantano, R. Qi, A. Rahnamoun, D.R. Roe, A. Roitberg, C. Sagui, S. Schott-Verdugo, J. Shen, C.L. Simmerling, N.R. Skrynnikov, J. Smith, J. Swails, R.C. Walker, J. Wang, H. Wei, R.M. Wolf, X. Wu, Y. Xue, D.M. York, S. Zhao, and P.A. Kollman (2021), Amber 2021, University of California, San Francisco.

[36] B.R. Brooks, C.L. Brooks III, A.D. Mackerell Jr, L. Nilsson, R.J. Petrella, B. Roux, Y. Won, G. Archontis, C. Bartels, S. Boresch, A. Caflisch, L. Caves, Q. Cui, A.R. Dinner, M. Feig, S. Fischer, J. Gao, M. Hodoscek, W. Im, K. Kuczera, T. Lazaridis, J. Ma, V. Ovchinnikov, E. Paci, R.W. Pastor, C.B. Post, J.Z. Pu, M. Schaefer, B. Tidor, R.M. Venable, H.L. Woodcock, X. Wu, W. Yang, D.M. York, M. Karplus, CHARMM: the biomolecular simulation program, J. Comput. Chem. 30 (2009) 1545-1614.

[37] K. Vanommeslaeghe, E. Hatcher, C. Acharya, S. Kundu, S. Zhong, J. Shim, E. Darian, O. Guvench, P. Lopes, I. Vorobyov, A.D. Mackerell Jr, CHARMM general force field: A force field for drug-like molecules compatible with the CHARMM all-atom additive biological force fields, J. Comput. Chem. 31 (2010) 671-690.

[38] M. Christen, P.H. Hünenberger, D. Bakowies, R. Baron, R. Bürgi, D.P. Geerke, T.N. Heinz, M.A. Kastenholz, V. Kräutler, C. Oostenbrink, C. Peter, D. Trzesniak, W.F. van Gunsteren, The GROMOS software for biomolecular simulation: GROMOS05, J. Comput. Chem. 26 (2005) 1719-1751.

[39] X. Wang, D.W. House, P.A. Oroskar, A. Oroskar, A. Oroskar, C.J. Jameson, S. Murad, Molecular dynamics simulations of the chiral recognition mechanism for a polysaccharide chiral stationary phase in enantiomeric chromatographic separations, Mol. Phys. 117 (2019) 3569-3588.

[40] R. Anandakrishnan, A. Drozdetski, R.C. Walker, A.V. Onufriev, Speed of conformational change: comparing explicit and implicit solvent molecular dynamics simulations, Biophys. J. 108 (2015) 1153-1164.

[41] G. Hu, M. Huang, C. Luo, Q. Wang, J.W. Zou, Interactions between pyrazole derived enantiomers and Chiralcel OJ: Prediction of enantiomer absolute configurations and elution order by molecular dynamics simulations, J. Mol. Graph. Model. 66 (2016) 123-132.

[42] R. Dallocchio, A. Dessì, M. Solinas, A. Arras, S. Cossu, E. Aubert, V. Mamane, P. Peluso, Halogen bond in high-performance liquid chromatography enantioseparations: Description, features and modelling, J. Chromatogr. A 1563 (2018) 71-81.

[43] R. Sardella, F. Ianni, L. Cossignani, G. Aldini, A. Carotti, Binding modes identification through molecular dynamic simulations: A case study with carnosine enantiomers and the Teicoplanin A2-2-based chiral stationary phase, J. Sep. Sci. 43 (2020) 1728-1736.

[44] L. Fumagalli, L. Pucciarini, L. Regazzoni, E. Gilardoni, M. Carini, G. Vistoli, G. Aldini, R. Sardella, Direct HPLC separation of carnosine enantiomers with two chiral stationary phases based on penicillamine and teicoplanin derivatives, J. Sep. Sci. 41 (2018) 1240-1246.

[45] X.Y. Meng, H.X. Zhang, M. Mezei, M. Cui, Molecular docking: a powerful approach for structure-based drug discovery, Curr. Computer-Aided Drug Design 7 (2011) 146-157.

[46] O. Trott, A.J. Olson, AutoDock Vina: improving the speed and accuracy of docking with a new scoring function, efficient optimization, and multithreading, J. Comput. Chem. 31 (2010) 455-461.

[47] X. Dou, X. Su, Y. Wang, Y. Chen, W. Shen, Studies on Pidotimod Enantiomers With Chiralpak-IA: Crystal Structure, Thermodynamic Parameters and Molecular Docking, Chirality 27 (2015) 802-808.

[48] I. Ali, A. Haque, Z.A. Al-Othman, A. Al-Warthan, L. Asnin, Stereoselective interactions of chiral dipeptides on amylose based chiral stationary phases, Sci. China Chem. 58 (2015) 519-525.

[49] I. Ali, D.R. Sahoo, Z.A. Al-Othman, A.A. Alwarthan, L. Asnin, B. Larsson, Validated chiral high performance liquid chromatography separation method and simulation studies of dipeptides on amylose chiral column, J. Chromatogr. A 1406 (2015) 201-209.

[50] I. Ali, M.N. Lone, M. Suhail, Z.A. AL-Othman, A. Alwarthan, Enantiomeric resolution and simulation studies of four enantiomers of 5-bromo-3-ethyl-3-(4-nitrophenyl)-piperidine-2, 6-dione on a Chiralpak IA column, RSC adv. 6 (2016) 14372-14380.

[51] D. Rossi, R. Nasti, S. Collina, G. Mazzeo, S. Ghidinelli, G. Longhi, M. Memo, S. Abbate, The role of chirality in a set of key intermediates of pharmaceutical interest, 3-aryl-substituted-γ-butyrolactones, evidenced by chiral HPLC separation and by chiroptical spectroscopies, J. Pharm. Biomed. Anal. 144 (2017) 41-51.

[52] B. Zhu, F. Zhao, J. Yu, Z. Wang, Y. Song, Q. Li, Chiral separation and a molecular modeling study of eight azole antifungals on the cellulose tris (3,5-dichlorophenylcarbamate) chiral stationary phase, New J. Chem. 42 (2018) 13421-13429.

[53] M. Li, B. Zhang, J. Yu, J. Wang, X. Guo, Enantiomeric separation and simulation study of eight anticholinergic drugs on an immobilized polysaccharide-based chiral stationary phase by HPLC, New J. Chem. 42 (2018) 11724-11731.

[54] L. Pisani, M. Rullo, M. Catto, M. de Candia, A. Carrieri, S. Cellamare, C.D. Altomare, Structure–property relationship study of the HPLC enantioselective retention of neuroprotective 7-[(1-alkylpiperidin-3-yl) methoxy] coumarin derivatives on an amylose-based chiral stationary phase, J. Sep. Sci. 41 (2018) 1376-1384.

[55] I. Ali, M. Suhail, L. Asnin, Chiral separation and modeling of quinolones on teicoplanin macrocyclic glycopeptide antibiotics CSP, Chirality 30 (2018) 1304-1311.

[56] L. Zhao, J. Xie, F. Guo, K. Liu, Enantioseparation of napropamide by supercritical fluid chromatography: effects of the chromatographic conditions and separation mechanism, Chirality 30 (2018) 661-669.

[57] Y. Zhao, S. Li, X. Wang, J. Yu, Y. Song, X. Guo, Enantioseparation and molecular modeling study of five β-adrenergic blockers on Chiralpak IC column, Chirality 31 (2019) 502-512.

[58] L.A. Papp, M. Foroughbakhshfasaei, B. Fiser, P. Horváth, E. Kiss, K. Sekkoum, Á. Gyéresi, G. Hancu, B. Noszál, Z.I. Szabó, G. Tóth, Reversed-phase HPLC enantioseparation of pantoprazole using a teicoplanin aglycone stationary phase—Determination of the enantiomer elution order using HPLC-CD analyses, Chirality 32 (2020) 158-167.

[59] M. Shahnani, Y. Sefidbakht, S. Maghari, A. Mehdi, H. Rezadoost, A. Ghassempour, Enantioseparation of mandelic acid on vancomycin column: Experimental and docking study, Chirality 32 (2020) 1289-1298.

[60] L. Cai, M. Xue, J. Lun, S. Li, J. Yu, X. Guo, Enantioseparation and molecular modeling study of eight psychoactive drugs on a coated polysaccharide-based chiral stationary phase, Electrophoresis 41 (2020) 2092-2101.

[61] R. Put, Y. Vander Heyden, Review on modelling aspects in reversed-phase liquid chromatographic quantitative structure–retention relationships, Anal. Chim. Acta 602 (2007) 164-172.

[62] C. Roussel, P. Piras, Chirbase: A molecular database for storage and retrieval of chromatographic chiral separations, Pure & Appl. Chem. 65 (1993) 235-244.

[63] R. Sheridan, W. Schafer, P. Piras, K. Zawatzky, E.C. Sherer, C. Roussel, C.J. Welch, Toward structure-based predictive tools for the selection of chiral stationary phases for the chromatographic separation of enantiomers, J. Chromatogr. A 1467 (2016) 206-213.

[64] M. Vitha, P.W. Carr, The chemical interpretation and practice of linear solvation energy relationships in chromatography, J. Chromatogr. A 1126 (2006) 143-194.

[65] H. Moriwaki, Y.S. Tian, N. Kawashita, T. Takagi, Mordred: a molecular descriptor calculator, J. Cheminform. 10 (2018) 4.

[66] R.I. Amos, P.R. Haddad, R. Szucs, J.W. Dolan, C.A. Pohl, Molecular modeling and prediction accuracy in Quantitative Structure-Retention Relationship calculations for chromatography, Trends Anal. Chem. 105 (2018) 352-359.

[67] C. West, G. Guenegou, Y. Zhang, L. Morin-Allory, Insights into chiral recognition mechanisms in supercritical fluid chromatography. II. Factors contributing to enantiomer separation on tris-(3,5-dimethylphenylcarbamate) of amylose and cellulose stationary phases, J. Chromatogr. A 1218 (2011) 2033-2057.

[68] J. Aires-de-Sousa, J. Gasteiger, New Description of Molecular Chirality and Its Application to the Prediction of the Preferred Enantiomer in Stereoselective Reactions, J. Chem. Inf. Comput. Sci. 41 (2001) 369-375.

[69] S. Caetano, J. Aires-de-Sousa, M. Daszykowski, Y. Vander Heyden, Prediction of enantioselectivity using chirality codes and classification and regression trees, Anal. Chim. Acta 544 (2005) 315-326.

[70] A. Del Rio, J. Gasteiger, Encoding Absolute Configurations with Chiral Enantiophore Descriptors. Application to the Order of Elution of Enantiomers in Liquid Chromatography, QSAR Comb. Sci. 27 (2008) 1326-1336.

[71] M. Dervarics, F. Ötvös, T.A. Martinek, Development of a chirality-sensitive flexibility descriptor for 3+ 3D-QSAR, J. Chem. Inf. Model. 46 (2006) 1431-1438.

[72] Y. Marrero-Ponce, F. Torrens, R. García-Domenech, S.E. Ortega-Broche, V.R. Zaldivar, Novel 2D TOMOCOMD-CARDD molecular descriptors: atom-based stochastic and non-stochastic bilinear indices and their QSPR applications, J. Math. Chem. 44 (2008) 650-673.

[73] J.R. Valdés-Martiní, Y. Marrero-Ponce, C.R. García-Jacas, K. Martinez-Mayorga, S.J. Barigye, Y.S.V. d'Almeida, H. Pham-The, F. Pérez-Giménez, C.A. Morell, QuBiLS-MAS, open source multi-platform software for atom-and bond-based topological (2D) and chiral (2.5 D) algebraic molecular descriptors computations, J. Cheminform. 9 (2017) 35.

[74] Y. Marrero-Ponce, J.A. Castillo-Garit, E.A. Castro, F. Torrens, R. Rotondo, 3D-chiral (2.5) atom-based TOMOCOMD-CARDD descriptors: theory and QSAR applications to central chirality codification, J. Math. Chem. 44 (2008) 755-786.

[75] H. Barfeii, Z. Garkani-Nejad, A comparative QSRR study on enantioseparation of ethanol ester enantiomers in HPLC using multivariate image analysis, quantum mechanical and structural descriptors, J. Chin. Chem. Soc. 64 (2017) 176-187.

[76] P. Ravisankar, S. Anusha, K. Supriya, U.A. Kumar, Fundamental chromatographic parameters, Int. J. Pharm. Sci. Rev. Res. 55 (2019) 46-50.

[77] P. Piras, R. Sheridan, E.C. Sherer, W. Schafer, C.J. Welch, C. Roussel, Modeling and predicting chiral stationary phase enantioselectivity: An efficient random forest classifier using an optimally balanced training dataset and an aggregation strategy, J. Sep. Sci. 41 (2018) 1365-1375.

[78] Y. Martín-Biosca, L. Escuder-Gilabert, M.J. Medina-Hernández, S. Sagrado, Modelling the enantioresolution capability of cellulose tris (3, 5-dichlorophenylcarbamate) stationary phase in reversed phase conditions for neutral and basic chiral compounds, J. Chromatogr. A 1567 (2018) 111-118.

[79] S. Khater, C. West, Characterization of three macrocyclic glycopeptide stationary phases in supercritical fluid chromatography, J. Chromatogr. A 1604 (2019) 460485.

[80] C. Luo, G. Hu, M. Huang, J. Zou, Y. Jiang, Prediction on separation factor of chiral arylhydantoin compounds and recognition mechanism between chiral stationary phase and the enantiomers, J. Mol. Graph. Model. 94 (2020) 107479.

[81] T.D. Booth, K. Azzaoui, I.W. Wainer, Prediction of chiral chromatographic separations using combined multivariate regression and neural networks, Anal. Chem. 69 (1997) 3879-3883.

[82] T.D. Booth, I.W. Wainer, Investigation of the enantioselective separations of α-alkylarylcarboxylic acids on an amylose tris (3,5-dimethylphenylcarbamate) chiral stationary phase using quantitative structure-enantioselective retention relationships Identification of a conformationally driven chiral recognition mechanism, J. Chromatogr. A 737 (1996) 157-169.

[83] C.A. Montanari, Q.B. Cass, M.E. Tiritan, A.L.S. de Souza, A QSERR study on enantioselective separation of enantiomeric sulphoxides, Anal. Chim. Acta 419 (2000) 93-100.

[84] M. Szaleniec, A. Dudzik, M. Pawul, B. Kozik, Quantitative structure enantioselective retention relationship for high-performance liquid chromatography chiral separation of 1-phenylethanol derivatives, J. Chromatogr. A 1216 (2009) 6224-6235.

[85] K. Boronová, J. Lehotay, K. Hroboňová, D.W. Armstrong, Study of physicochemical interaction of aryloxyaminopropanol derivatives with teicoplanin and vancomycin phases in view of quantitative structure–property relationship studies, J. Chromatogr. A 1301 (2013) 38-47.

[86] B. Rasulev, M. Turabekova, M. Gorska, K. Kulig, A. Bielejewska, J. Lipkowski, J. Leszczynski, Use of quantitative structure–enantioselective retention relationship for the liquid chromatography chiral separation prediction of the series of pyrrolidin-2-one compounds, Chirality 24 (2012) 72-77.

[87] V. Svetnik, A. Liaw, C. Tong, J.C. Culberson, R.P. Sheridan, B.P. Feuston, Random forest: a classification and regression tool for compound classification and QSAR modeling, J. Chem. Inf. Comput. Sci. 43 (2003) 1947-1958.

[88] R.E. Carhart, D.H. Smith, R. Venkataraghavan, Atom pairs as molecular features in structure-activity studies: definition and applications, J. Chem. Inf. Comput. Sci. 25 (1985) 64-73.

[89] S.K. Kearsley, S. Sallamack, E.M. Fluder, J.D. Andose, R.T. Mosley, R.P. Sheridan, Chemical similarity using physiochemical property descriptors, J. Chem. Inf. Comput. Sci. 36 (1996) 118-127.

[90] S. Vilar, G. Cozza, S. Moro, Medicinal chemistry and the molecular operating environment (MOE): application of QSAR and molecular docking to drug discovery, Curr. Top. Med. Chem. 8 (2008) 1555-1572.

[91] G. Cruciani, P. Crivori, P.A. Carrupt, B. Testa, Molecular fields in quantitative structure–permeation relationships: the VolSurf approach, J. Mol. Struct. 503 (2000) 17-30.

[92] G. Cruciani, M. Pastor, R. Mannhold, Suitability of molecular descriptors for database mining. A comparative analysis, J. Med. Chem. 45 (2002) 2685-2694.

[93] M. Pérez-Baeza, L. Escuder-Gilabertt, Y. Martín-Biosca, S. Sagrado, M.J. Medina-Hernández, Comparative modelling study on enantioresolution of structurally unrelated compounds with amylose-based chiral stationary phases in reversed phase liquid chromatography-mass spectrometry conditions, J. Chromatogr. A 1625 (2020) 461281.

[94] S. Khater, Y. Zhang, C. West, Insights into chiral recognition mechanism in supercritical fluid chromatography III. Non-halogenated polysaccharide stationary phases, J. Chromatogr. A 1363 (2014) 278-293.

[95] C. West, Y. Zhang, L. Morin-Allory, Insights into chiral recognition mechanisms in supercritical fluid chromatography. I. Non-enantiospecific interactions contributing to the retention on tris-(3,5-dimethylphenylcarbamate) amylose and cellulose stationary phases, J. Chromatogr. A 1218 (2011) 2019-2032.

[96] A. Berthod, C.R. Mitchell, D.W. Armstrong, Could linear solvation energy relationships give insights into chiral recognition mechanisms?: 1. π–π and charge interaction in the reversed versus the normal phase mode, J. Chromatogr. A 1166 (2007) 61-69.

[97] C.R. Mitchell, D.W. Armstrong, A. Berthod, Could linear solvation energy relationships give insights into chiral recognition mechanisms?: 2. Characterization of macrocyclic glycopeptide stationary phases, J. Chromatogr. A 1166 (2007) 70-78.

[98] S. Khater, Y. Zhang, C. West, Insights into chiral recognition mechanism in supercritical fluid chromatography IV. Chlorinated polysaccharide stationary phases, J. Chromatogr. A 1363 (2014) 294-310.